Proceedings of the 17th Pan-American Conference on Soil Mechanics and Geotechnical Engineering (XVII PCSMGE), and 2nd Latin-American Regional Conference of the International Association for Engineering Geology and the Environment (IAEG), La Serena Chile, 2024.

Enhancing dam safety: Seismic vulnerability assessment of Guavio dam

Mejoramiento de la seguridad de una presa: Evaluación de la vulnerabilidad sísmica de la presa Guavio

Camilo Marulanda[1] & William Ruíz[2].

1 Technical Manager, INGETEC, Bogotá, Colombia, marulanda@ingetec.com.co

2 Head of Dams Department, INGETEC, Bogotá, Colombia, wruiz@ingetec.com.co

ABSTRACT: This paper explores the seismic vulnerability of the 245-meter-high Guavio Dam, presenting a comprehensivegeotechnical analysis that includes limit equilibrium, simplified methods, and a finite element numerical model. This study aims to assess the dam's behavior and performance in light of the findings from the latest 2019 seismic hazard update, which increased the design seismic acceleration for an extreme maximum credible earthquake event from 0.26 g to 0.46 g.This increase is attributed to substantial changes in the available reference data, especially concerning the seismic catalog (historical and instrumental) and new attenuation laws. These factors significantly influence the definition of scenarios associated with the maximum credible earthquake and verification accelerations for the dam. Finite element models were constructed to analyze both the construction sequence and the dynamic behavior of the dam. Each model was calibrated against geotechnical instrumentation records for static conditions and geophysical test results from this study for dynamic conditions. The evaluation of the dam's dynamic behavior involved the use of simplified analysis methodologies and the development of three-dimensional finite element models. A sensitivity analysis was also conducted as part of the finite element modeling to investigate the impact of the dam's fundamental vibration periods on the magnitude of seismically induced deformations. The findings and methodologies detailed in this paper contribute to a thorough seismic vulnerability assessment of the Guavio Dam.

KEYWORDS: Enhancing dam safety, Guavio Dam, Earth Core Rockfill Dam, dynamic behavior of the dam.

1. INTRODUCTION.

The Guavio Dam, also known as the Guavio Dam, is an Earth-Core Rockfill Dam (ECRD) featuring an impermeable core, constructed between 1984 and 1989. Recent revisions to the basis for estimating the dam's seismic vulnerability, prompted by updates to the seismic analysis catalog (historical and instrumental) and the introduction of new attenuation laws, have led to significant changes. These updates have defined scenarios related to the maximum credible earthquake and verification accelerations for critical project infrastructure. The latest seismic hazard study, completed in 2019, indicates an increase in peak ground acceleration for extreme events, from 0.26g to 0.46g. Consequently, it is crucial to reassess the dam's behavior by updating the stability and seismic vulnerability analyses.

This paper outlines the analyses conducted to assess the dam's performance in light of the revised earthquake projections. This involved a comprehensive review and interpretation of the dam's instrumentation records and data from a supplementary geophysical campaign. From this data, a series of 2D and 3D slope stability analyses were performed using the Limit Equilibrium Method (LEM) and the Strength Reduction Method (SRM), considering varying reservoir levels. This was followed by a stress-strain analysis conducted in stages as part of the calibration process, and a dynamic analysis to estimate seismically induced deformations.

1.1. DESCRIPTION OF THE DAM

The Alberto Lleras Camargo Dam, part of the Guavio Hydroelectric Power Plant, stands as a 245-meter-high Earth Core Rockfill Dam (ECRD) on the Guavio River. Located 180 km from Bogotá D.C. in the municipality of Ubalá, Cundinamarca, the dam features a crest that is 14 meters wide and approximately 415 meters long. The upstream shell of the dam has an average slope of 2.00H:1V, while the downstream shell slopes at 1.80H:1V. Inter-ramp slopes average 1.40H:1V, with ramp widths varying between 9 and 15 meters and a maximum gradient of 14%. The dam's volume is approximately 17 million cubic meters. Constructed between 1984 and 1989, the dam comprises rockfill and a core of clayey material containing over 30% fines.

A significant feature of this dam is its comprehensive instrumentation system, operational since 1986, which facilitates the monitoring and analysis of the dam's behavior. This system includes topographic control points along the slopes and crest, horizontal and vertical movement recorders on the downstream shell, pneumatic settlement sensors, pressure cells in the core and downstream shell, and pneumatic piezometers in the core and foundation of the dam. Figures 1 and 2 illustrate the location of the instruments.

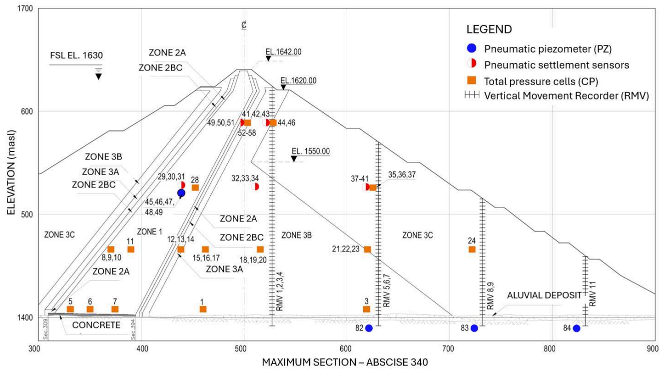

Figure 1. Instrumentation - Maximum Dam section.

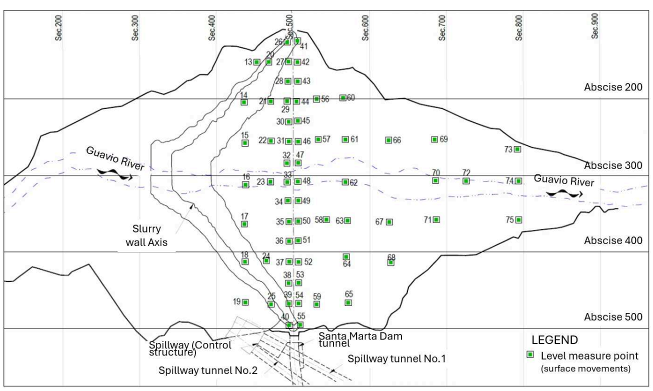

Figure 2. Topographic control points of the Alberto Lleras Dam

1.2. RESERVOIR BEHAVIOR

During the operational period of the reservoir, the lowest recorded level occurred on May 2, 2008, measuring at EL. 1556.5 masl. This level was 46.5 meters above the Minimum Operating Level, defined by the elevation of the intake of the power tunnel (refer to Figure 3). Notably, the reservoir exhibits an average rate of variation of approximately 1 meter per day. Interestingly, the rates of descent are observed to exceed those of ascent, with the most significant variations noted at the onset of 2018. During January 25 to January 28 of that year, for instance, the reservoir descended at an extraordinary rate of 6.17 meters per day, culminating in a total descent of 18 meters over three days.

In the two-dimensional (2D) Limit Equilibrium Method (LEM) analyses, a rapid drawdown scenario was considered, transitioning from the Maximum Operational Level (EL. 1630.0 masl) to EL. 1510.0 masl, which aligns with the lower level of the intake. It's crucial to note that this scenario represents an extreme condition. When considering submergence effects, the minimum reservoir level must exceed EL. 1510 masl to prevent air from entering the submerged powertunnel. Consequently, the rapid drawdown analyses represent conservative scenarios. The analyses assumed constant reservoir variation rates of 5.0 m/day and 10.0 m/day. These rates were established based on the observed reservoir decrease of 18 meters between January 25 and January 28, 2018, indicating a maximum historical rate of approximately 6 m/day.

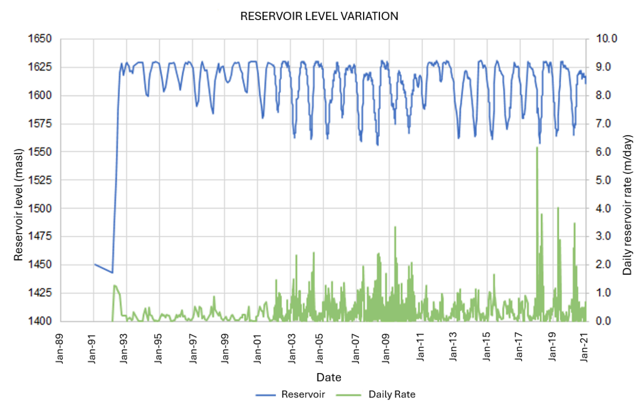

Figure 3. Reservoir level and rate of variation (fluctuation).

1.3. PIEZOMETRIC LEVELS

Figure 4 illustrates the pore pressures within the impermeable core at an elevation of 1523 masl, spanning between abscissae 230 and 410. Following the initial filling, there was a gradual dissipation of the excess pore pressures from 1992 through approximately 2007. The finite element models incorporate a rest period aimed at allowing the dissipation of these pore pressures, which facilitates an accurate representation of the dam’s current state. Based on this updated condition, subsequent analyses such as slope stability (using a 3D model with the Strength Reduction Method, SRM) and dynamic analyses are conducted to ensure ongoing structural integrity.

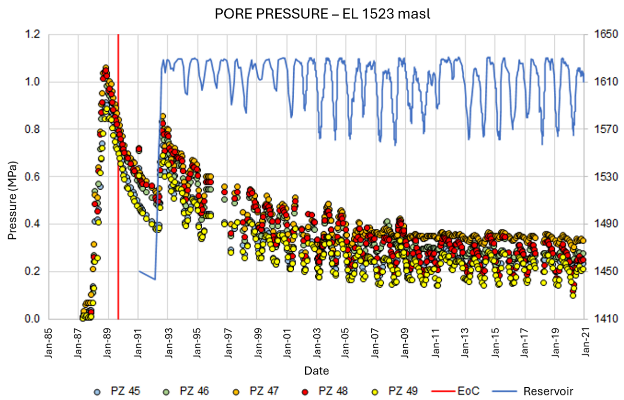

Figure 4. Pore pressures in impermeable core at EL. 1523 masl.

2. SEISMIC HAZARD

The seismic hazard assessment for the Guavio Hydroelectric Power Plant, conducted by INGETEC in 2019, identified the Safety Evaluation Earthquake (SEE) scenario for the Guavio Dam. This scenario is defined by a rock verification spectrum with a peak ground acceleration (PGA) of 0.46 g, a spectral acceleration on the platform or for periods shorter than the short period (Sa) of 1.15 g, and a short period (T1) of 0.35 seconds.

In Colombia, where specific codes, standards, or regulations regarding dam safety are absent, this study adhered to the guidelines from Bulletin 148 ICOLD, "Selecting Seismic Parameters for Large Dams - Guidelines (revision of Bulletin 72)", particularly the provisions of Section 3.4. This section deals with accelerograms, verification spectra, and PGA, and is critical given the potentially severe to extreme consequences of a failure at the Guavio Dam. Consequently, the verification earthquake was established using the 84th percentile for deterministic analysis.

Figure 5 illustrates the verification spectrum for a scenario involving a cortical earthquake on the Santa Maria fault, with a magnitude of Mw = 6.8 and an epicentral distance of 8.0 km. The Santa María fault, part of the Eastern Fault System with a reverse mechanism, extends over 93 km. Notably, the determination of the verification spectrum diverges from the original design analyses due to advancements in attenuation laws for cortical events, which have been a significant focus of research over the past 40 years.

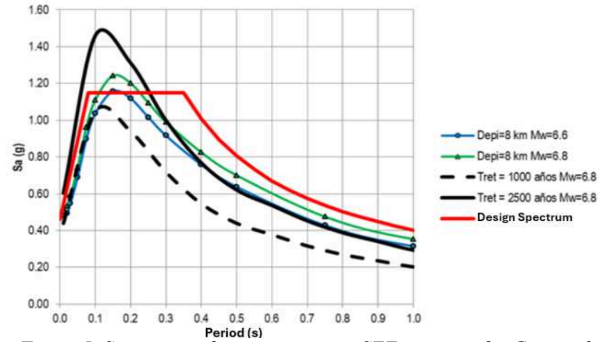

Figure 5. Seismic verification spectrum SEE scenario for Guavio dam.

In this study's nonlinear dynamic analyses, six sets of ground motions—each comprising one horizontal and one vertical component—were selected. These ground motions were recorded on rock sites impacted by reverse mechanism faults, with magnitudes (Mw) close to 6.8 and epicentral distances of less than 30.0 km. Specifically, the selected records come from the Chuetsu, San Fernando, Loma Prieta, Northridge, and Iwate earthquakes. These events are considered representative of the seismic hazard at the study site. When scaled, their response spectra closely align with the proposed verification or analysis spectrum, as demonstrated in Figure 6.

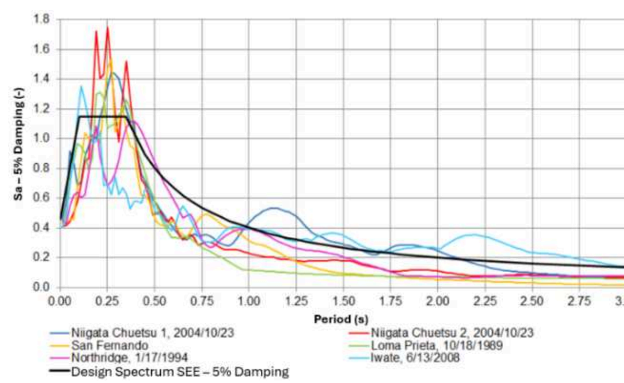

Figure 6. Comparison of the response spectra of the selected ground motions and the SEE seismic verification spectrum.

3. GEOPHYSICAL EXPLORATION CAMPAIGN

For the assessment of dynamic analysis of seismic response, a geophysical exploration was proposed, through the development of MASW method (Multichannel Analysis of Surfaces Waves) and HVSR test (Horizontal Vertical Spectral Ratio).

The objective of the first test was to determine the shear wave velocities (VS) of the dam fill to estimate the shear stiffness modulus (G) for the dynamic analyses, while the HVSR test was used to estimate the fundamental period and the main vibration modes of the dam.

Figure 7 shows the shear wave velocities obtained for the 5 MASW tests and the proposed potential regression, with which a shear wave velocity of approximately 680 m/s can be estimated at a depth of 60 m, a representative depth for the Guavio dam (center of mass of a perfect tetrahedron).

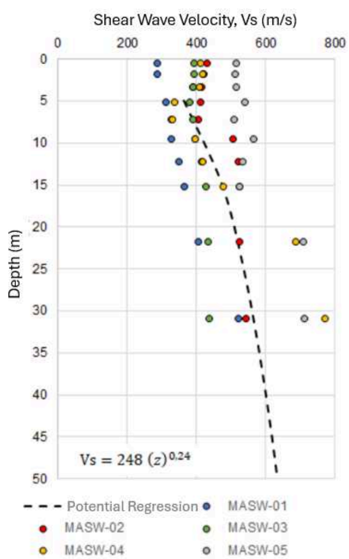

Figure 7. MASW test results and relationship between depth and shear wave velocity.

For the interpretation of the HVSR test data from the Guavio dam, the DEGTRA A4 software developed by researchers at the National Autonomous University of Mexico (UNAM) in 2005 (Ordaz et al.) was employed. Initially, the recorded ground motions signals underwent decimation, followed by a baseline correction for each ground motion using the algorithm implemented in the DEGTRA A4 program. Subsequently, the Fourier spectrum was calculated to determine the transfer functions between the component perpendicular to the dam axis and the vertical component (TFYX), as well as between the component parallel to the dam axis and the vertical component (TFZX).

To define the predominant period of the dam, the maximum peak of the transfer function was identified within the frequency range of 0.33 Hz (3.0 seconds) to 1 Hz (1.0 second). This frequency range captures the fundamental period of the dam, considering the height characteristics and the stiffness at low deformations of the materials composing the dam. Figure 8 illustrates the transfer functions for HVSR-08 using a decimation of 10. Due to the significant variation in the estimated fundamental periods using this methodology, the median of the five environmental noise records was chosen as a representative value. This approach estimated a fundamental period of 2.05 seconds and 2.50 seconds for the TFYX transfer function (direction perpendicular to the dam axis where the first vibration mode occurs) with decimations of 10 and 15, respectively.

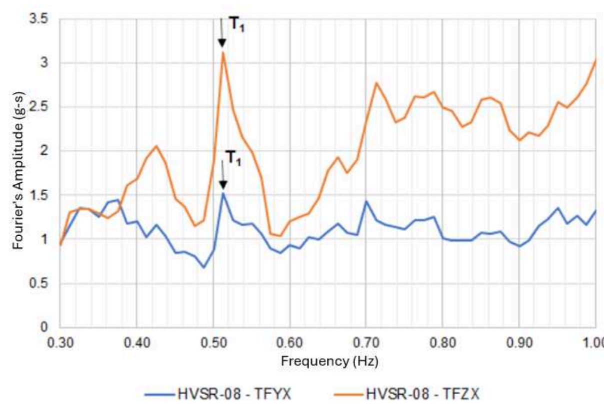

Figure 8. Transfer functions in register GVSR-08.

Based on the shear wave velocities derived from the MASW tests and the fundamental periods estimated using the environmental noise tests via the Nakamura (1989) technique, also known as HVSR (Mucciarelli and Gallipoli, 2004), it was deemed appropriate to incorporate a range of sensitivity in the fundamental period for the dynamic analyses. We considered T1 values of 1.75 s, 2.00 s, and 2.50 s. This approach allows us to manage the uncertainties associated with this property and to enhance the robustness of predictions regarding potential settlements the dam might experience under the impact of the design earthquake.

4. SLOPE STABILITY ANALYSIS

4.1. TWO-DIMENSIONAL ANALYSIS (LEM)

Two-dimensional analyses were performed for the maximum section of the dam. Figure 9 presents this section with the zoning used for stability analyses, where it is considered that this includes all areas of the dam and the shell backrests with their corresponding inter-ramp slopes.

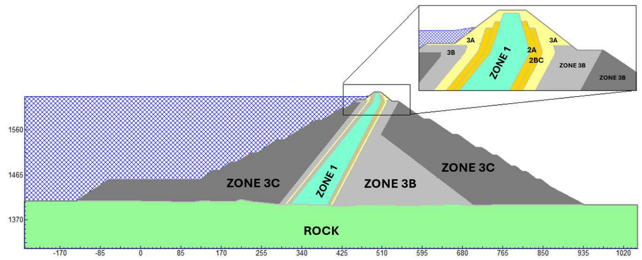

Figure 9. 2-D Model for Limit Equilibrium Method - LEM

The resistance criteria for the core and transition zones of the Guavio dam are based on the Mohr-Coulomb envelope, utilizing parameters detailed in Table 1, which were established during the material characterization phase. For the resistance of the enclosures (Zones 3A, 3B, and 3C), a non-linear resistance envelope was used, representative of the reference triaxial tests (Silva and Marsal, 1970). Figure 10 displays a comparison of non-linear resistance envelopes (Barton, 2016) against laboratory tests, illustrating that the envelope best fitting the dam's enclosures is the resistance envelope for medium rockfills (red curve in Figure 10). This particular resistance profile was applied in the two-dimensional stability analyses conducted via limit equilibrium methods.

Table 1. Geotechnical parameters for two-dimensional analysis.

Material	γ (kN/m³)	k (m/s)	Strength Parameters	
			Cohesion c' (kPa)	Friction φ (°)
Rockfill 3A and 3B	22,5	$5x10^{-1}$ $5x10^{-2}$	Nonlinear envelope	
Rockfill 3C	22,5	$1x10^{-1}$ $1x10^{-2}$	Nonlinear envelope	
Transition and filters (2A-2B)	21,0	$1x10^{-3}$	0	38
Core (Zone 1)	22,0	$1x10^{-8}$ $1x10^{-9}$	30	21

Due to the disparity in rigidity and resistance between the dam body and its foundation, which consists of moderately weathered Paleozoic rocks, a Mohr-Coulomb resistance model was employed for the foundation material. This model specifies a cohesion of 500 kPa and a friction angle of 45°. These parameters were selected to prevent failures through the foundation rock, as such occurrences are not anticipated given the type of materials encountered during the construction phase. This approach ensures that the foundation's integrity aligns with the expected conditions and material characteristics.

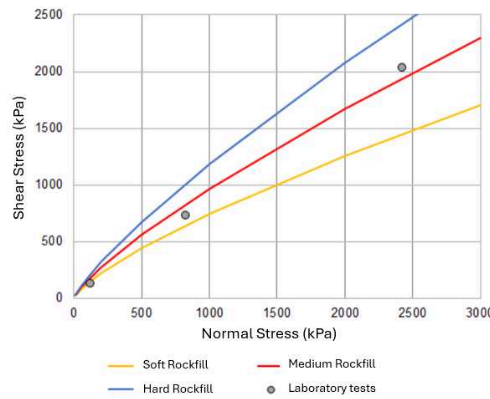

Figure 10. Nonlinear envelopes - Rockfill Triaxial Tests comparison.

Static slope stability was assessed under two water table conditions within the dam, determined through a flow analysis conducted using the finite element method. This analysis considered two scenarios: one with the reservoir at the Full reservoir Level (FSL) corresponding to EL. 1630 masl, and another with the water level at the lower elevation of the intake site (EL. 1510 masl). Figure 11 displays the results of these flow analyses in terms of total hydraulic head. The findings indicate that under the FSL condition, the piezometric levels near piezometers PZ-82 to PZ-84 closely match the values recorded by these instruments, demonstrating the accuracy of the flow analysis in reflecting actual conditions.

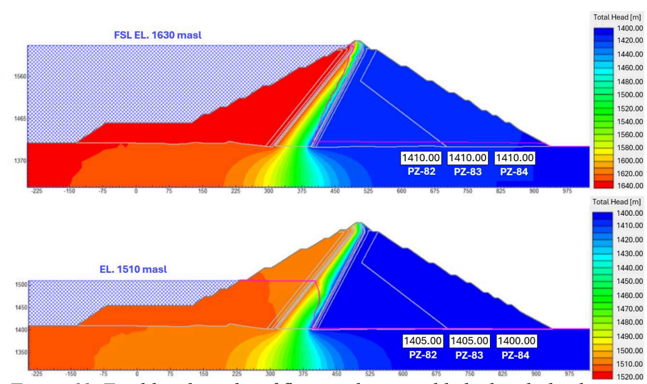

Figure 11. Total head results of flow analysis established with the dam level in the EL. 1630 masl and 1510 masl.

In addition to evaluating static stability under two water table conditions as shown in Figure 11, the stability of the dam was also assessed following a rapid drawdown from EL. 1630 masl to EL. 1510 masl, with drawdown rates of 5 m/day and 10 m/day. These rates were chosen based on the maximum observed drawdown rate of 6 m/day during the project's operation. The pore pressure conditions for these analyses were determined using a transient flow analysis with the aforementioned drawdown rates, incorporating a sensitivity analysis for permeability.

The dynamic stability of the dam was evaluated through pseudo-static analyses, using the pore pressure states derived from the flow analyses at the Full Supply Level (FSL), as shown in Figure 11. These slope stability analyses were conducted using Rocscience's SLIDE 2D Software, which employs the Limit Equilibrium Method (LEM) utilizing Spencer's methodology of slices. This method accounts for both force and moment balance equations, providing a more reliable estimation of safety factors.

4.1.1. *Static stability with steady state flow in the FSL*

The global and inter-ramp safety factors obtained meet the recommended minimum values. These safety factors are summarized in Table 2.

Table 2. Static stability results with flow established in the FSL - Two-Dimensional Analysis.

Case	Upstream Slope	Downstream Slope
	(Global >= 1,50)	**(Global >= 1,50)**
	(Inter-ramp >= 1,40)	**(Inter-ramp >= 1,40**
Global	2,42	1,97
Inter-ramp	> 2,42	> 1,97

4.1.2. *Static stability with steady state flow in the EL. 1510 masl*

In these analyses it is appreciated that with the lowest level of the dam the stability of the upstream shell up to a safety factor of 1.79, while the stabilities of the downstream slope increase slightly compared to the stabilization when the valley is in the FSL.

Table 3. Static stability results with flow established in the EL. 1510 masl - Two-Dimensional Analysis.

Case	Upstream Slope	Downstream Slope
	(Global >= 1,50)	**(Global >= 1,50)**
	(Inter-ramp >= 1,40)	**(Inter-ramp >= 1,40**
Global	1,79	1,99
Inter-ramp	> 1,79	> 1,99

4.1.3. *Static stability after rapid drawdown*

For all the assessed conditions the minimum safety factor is met and that in addition the variation of the safety factors with permeability and the rate of unpacking is practically zero, which suggests that given the materials that make up the Guavio dam and the possible rates for drawdown, the possibility that problems of instability by rapid drawdown are presented is minimal.

Table 4. Static stability results after rapid drawdown.

Case	Rate of 5 m/day	Rate of 10 m/day
	(Global >= 1,50)	**(Global >= 1,50)**
	(Inter-ramp >= 1,40)	**(Inter-ramp >= 1,40**
Global	1,71	1,71
Inter-ramp	1,71	1,71

4.1.4. *Dynamic stability (Pseudo-Static Analysis) with steady state flow in FSL*

For the Guavio Dam site, the acceleration of the evaluation earthquake, which serves as the equivalent inertial force for this analysis, is set at 0.23 g. This value represents 50% of the estimated maximum horizontal acceleration in rock (PGA = 0.46 g) for the maximum verification seismic force. Additionally, a vertical component of the seismic force, equivalent to two-thirds of the horizontal component, was also considered; this equates to a vertical acceleration of 0.153 g applied upwards. This adjustment follows the recommendations by Bozorgnia and Campbell (2004) concerning the relationship between the PGA of vertical and horizontal components for a low cortical earthquake at a given epicentral distance. The safety factors obtained from this analysis are all greater than 1.0, indicating compliance with the minimum safety criteria for this type of analysis. For the authors, the criterion of a pseudo-static safety factor for evaluating a dam of these characteristics is not suitable, and it is considered that a deformation criterion is the appropriate assessment for this type of structures under seismic loads (Marulanda 2023).

Table 5. Static stability results after rapid drawdown.

Case	Upstream Slope	Downstream Slope
	(Global >= 1,50)	**(Global >= 1,50)**
	(Inter-ramp >= 1,40)	**(Inter-ramp >= 1,40**
Global	1,04	1,22
Inter-ramp	> 1,04	> 1,22

4.2. THREE-DIMENSIONAL ANALYSIS (LEM)

Three-dimensional stability analyses were conducted for both the upstream and downstream slopes of the dam, considering the reservoir at its maximum ordinary water level (FSL - EL. 1630 masl) and assuming potential failure surfaces in an ellipsoidal shape. These slope stability analyses utilized the CLARA-W software [Hungr, (2001)], implementing the limit equilibrium method and employing the Bishop and Spencer methods adapted to three-dimensional border equilibrium [Cheng and Yip (2007), Huang et al., (2002), and Hungr (1994)]. These adaptations extend the traditional slice formulation to 3D volumetric column elements.

The geometry of the dam is depicted in Figure 12, which illustrates the configuration of the abutments based on the reconstructed topography and details of the upstream and downstream slopes, including access ramps. Due to the limitations of the CLARA-W software, which does not support the inclusion of a non-linear resistance envelope, the analyses were performed using three different scenarios of Mohr-Coulomb model resistance parameters. These scenarios were derived from the reference triaxial tests and included: a friction angle of 40° with a cohesion of 30 kPa, a second scenario with a 43° friction angle and 5 kPa cohesion, and a sensitivity analysis for a fully frictional Mohr-Coulomb type material with 0 kPa cohesion and a friction angle ranging from 38° to 46°.

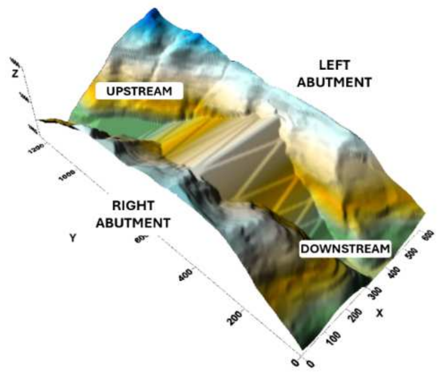

Figure 12. 3D geometry for Slope Analysis with LEM.

The pore pressures in this model were considered using a surface that marks the piezometric level. This surface was defined from a three-dimensional extrapolation of the surface obtained in the established flow analyses of the two-dimension equilibrium model. With this three-dimensional model, the following analyses were carried out for both slopes of the dam:

- Static stability with steady state flow for level reservoir in FSL (EL. 1630 masl).
- Pseudo-static analysis with steady state flow for level reservoir in FSL and horizontal acceleration coefficient k_h equal to half the PGA value defined in the seismic threat study developed in 2019, i.e. a k_h=0.23 g.

The results of upstream slope analysis are presented in Table 6 and the results of downstream slope analysis are presented in Table 7. The safety factors obtained with the expected resistance parameters in the rockfill shells are higher than the recommended minimum value for both the inter-ramp hole and the overall stability of the back, thus meeting the current safety criteria for this type of dams.

Table 6. Results 3D Upstream Slope Analysis - Guavio Dam.

Analysis No	**Rockfill strength**	**Upstream slope**	**Mobilized material. Vol. (m^3)**	**FSL (EL. 1630 masl)**	
				FS Static	**FS Pseudo**
				(Global >= 1,50)	**(K_h = 0,23 g)**
				(Inter-ramp >= 1,40)	**(FS >= 1,0)**
1	c' = 30 kPa φ' = 40°	Global	1.235.000	2,17	1,38
		Inter-ramp	244.000	2,50	1,55
2	c' = 5 kPa φ' = 43°	Global	1.450.000	2,28	1,42
		Inter-ramp	115.600	2,18	1,33
3	c' = 0 kPa φ' = 38° - 46°	Global	1.815.000	1,90 -2,52	1,19 - 1,60
		Inter-ramp	20.300	1,65 - 2,17	1,00 - 1,31

Table 7. Results 3D Downstream Slope Analysis - Guavio Dam.

Analysis No	**Rockfill strength**	**Downstream slope**	**Mobilized material. Vol. (m^3)**	**FSL (EL. 1630 masl)**	
				FS Static	**FS Pseudo**
				(Global >= 1,50)	**(K_h = 0,23 g)**
				(Inter-ramp >= 1,40)	**(FS >= 1,0)**
1	c' = 30 kPa φ' = 40°	Global	1.060.000	2,21	1,40
		Inter-ramp	120.000 - 300.000	1,96 - 2,05 - 2,23	1,24 - 1,35
2	c' = 5 kPa φ' = 43°	Global	995.000	2,33	1,47
		Inter-ramp	122.000 - 360.000	2,04 - 2,08 - 2,13	1,29 - 1,32 - 1,36
3	c' = 0 kPa φ' = 38° - 46°	Global	475.000 - 940.000	2,11 - 2,79	1,33 - 1,76
		Inter-ramp	278.000	1,59 - 2,10	1,01 - 1,33

4.3. THREE-DIMENSIONAL ANALYSIS (SRM)

In addition to previous analyses, the stability of the dam was further evaluated using the Strength Reduction Method (SRM) with the Drucker Prager Cap model in the multipurpose software Abaqus. Figure 13 displays the magnitude of total deformation, incorporating all three components, for a resistance reduction factor of 1.8. This clearly shows a failure mechanism on the upstream slope. The results are satisfactorily consistent with the Safety Factor outcomes from the three-dimensional assessment of boundary equilibrium. This congruence provides additional validation that the dam maintains adequate safety levels.

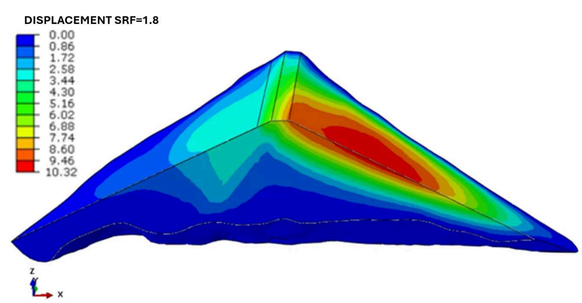

Figure 13. Displacements for SRF=1.8.

5. CONSTRUCTION AND FIRST RESERVOIR STAGES WITH STRAIN-STRES ANALYSIS (FEM)

The model of the construction of the Guavio dam consists of the sequential activation of layers of material following the constructive steps by a Soils Consolidation type analysis in Abaqus. This analysis considers the coupling between pore pressure and effective stress, establishing the equilibrium in terms of total stress.

During the construction of the dam, the rockfills are kept unsaturated above the phreatic level (EL. 1410 masl), and the effect of negative porous pressure on effective stress is limited by saturation, according to the principle of effective stress.

Figure 14 shows the state of pore pressure at the end of the dam construction in August 1989.

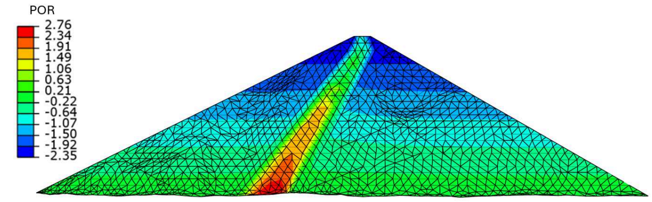

Figure 14. Pore pressure distribution at the end of the dam construction in August 1989.

To evaluate dynamic and stability slope analyses considering the proper strength and stiffness of the materials, this model includes a rest period during which excess pore pressure is dissipated, until the node corresponding to the PZ-48 piezometer presents a pressure of 0.31 MPa (see Figure 15).

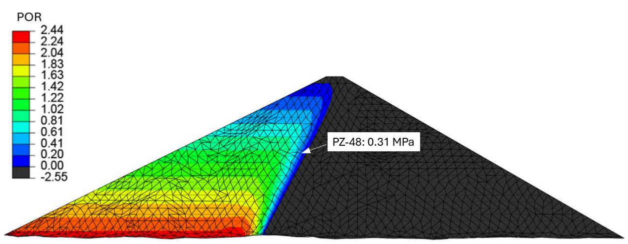

Figure 15. Pore pressure distribution with reservoir at EL. 1630 masl at the end of rest period.

6. VALIDATION OF THE 3D NUMERIC MODEL FROM THE GEOTECHNICAL INSTRUMENTATION

To validate the compressibility parameters of each dam material, the non-linear stiffness parameters of the Drucker Prager Cap model were calibrated based on the settlements observed at the end of the construction of the downstream shell. Figure 16 displays the settlements recorded at the end of construction using vertical movement recorders (VMRs), alongside the modeled settlement results depicted in continuous lines. A close correlation is observed both in the shape of the settlements and in their magnitude, indicating a good match between the observed data and the model predictions.

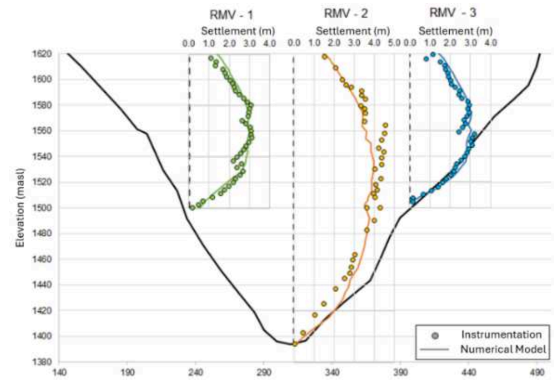

Figure 16. Comparison of settlements of the calibrated numerical model with VMRs of Section 535.

7. DYNAMIC ANALYSIS FOR ESTIMATING SEISMICALLY INDUCED DEFORMATIONS

As a first estimate, the Makdisi and Seed (1979) simplified method was used with the six analytical ground motions presented in Section 2., and the yield accelerations obtained for the upper backrest (critical condition). The estimated maximum displacements for the current condition of the Guavio dam are obtained for the Chuetsu 1 and Northridge input ground motions with values of 25.9 cm, 81.6 cm and 117.1 cm for a cutting wave velocities of 450 m/s, 550 m/s and 650 m/s, respectively. The established cutting velocities guarantee fundamental mean periods between the six ground motions between 1.76 s and 2.62 s, values that are within the estimated range of periods defined from the geophysical tests carried out. Based on the results, numerical time-dependent modelling was carried out for the signals of Niigata Chuetsu 1, Northridge and Iwate, considering that for these three ground motions the highest shifts were obtained for the low, medium and high rigidity models.

7.1. NUMERICAL MODEL

The numerical model for dynamic analyses starts from a state of stresses and pore pressures that approaches the state of the dam after dissipating the pore pressures of the core and corresponding to the reservoir level at the EL 1630 masl.

The dynamic model includes the hydrodynamic effect of the dam using the Westergaard grouped mass methodology, with the generalization for inclined walls defined by Zangar (1952).

Figure 18 shows the variation of the mass per unit of area for the level of the dam at the FSL (EL. 1630 masl) and 1,3H:1,0V slope (maximum inter-ramp slope), for comparison this Figure includes the mass by unit of surface determined with the original formulation of Westergaard (vertical walls) and the mass for unit area equivalent to a hydrostatic pressure.

The analysis of the frequency content of the six ground motions in terms of the Fourier spectrum is presented in Figure 19.

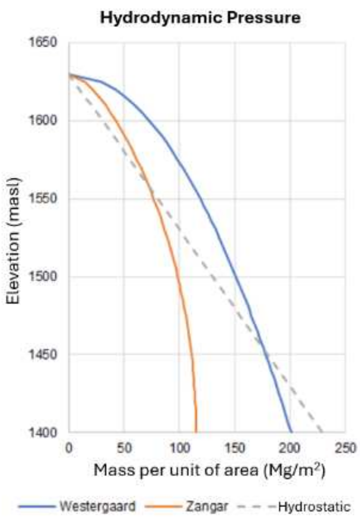

Figure 18. Hydrodynamic pressure comparison.

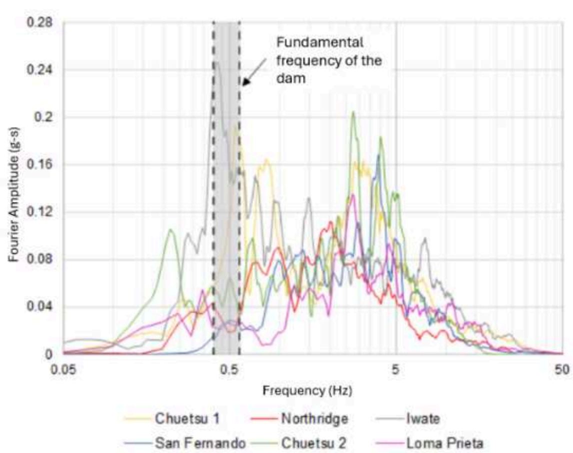

Figure 19. Fourier Spectral Analysis Ground Motions.

1.1. MODAL ANALYSIS AND MODEL CALIBRATION

The calibration of the numerical model for the estimation of earthquake-induced deformations was based on calibrating the model's fundamental period to coincide with the estimated fundamental period by geophysical tests, which suggest that the fundamental period of the dam is between 1.75 s and 2.50 s.

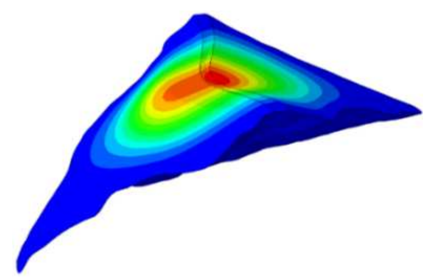

Figure 20. First vibration mode for Guavio Dam.

Figure 20 shows the deformation of the beam for the first vibration mode, for the calibration of this fundamental period it was necessary to adjust the rigidity of the model, of the elastic modules that control the discharge in the Drucker-Prager Cap model. Table 8 presents the values of these calibrated modules for different prey materials for periods of 1.75 s, 2.00 s and 2.50 s.

The results of the dynamic numerical model with the Iwate ground motion were used to evaluate the base period of the dam with the transfer function between the horizontal acceleration signal on the crevice and the Horizontal Acceleration Signal at the base of the model. The transfer functions for models with compressibility parameters that guarantee periods of 1.75 s, 2.00 s and 2.50 s are presented in Figure 21. The transfer function peaks of each model correspond approximately to the periods estimated in the modal analysis.

The hardening curves of the materials were adjusted so that all models used in the analysis adequately represented the settlements during the dam construction period, i.e. that they were calibrated with the dam instrumentation.

Table 8. Dynamic elastic modulus calibrated for the dynamic model.

Material	Young Modulus (MPa)		
	T1 = 1,75 s	T1 = 2,0 s	T1 = 2,5 s
Core	96	72	48
Filter	192	144	96
3B	416	312	208
3C	416	312	208

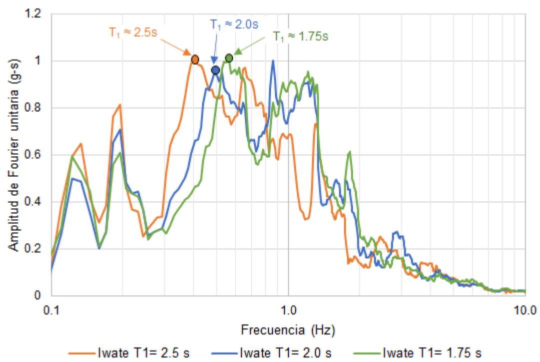

Figure 21. Transfer functions for the Iwate earthquake.

1.2. DAMPING

The model incorporated viscous Rayleigh damping, which is dependent on frequency. We adhered to the guidelines set forth by Hudson et al. (1994), which recommend setting the first frequency equal to the base frequencies of the dam—specifically 1.75 s, 2.00 s, and 2.50 s. This approach ensures that the damping rate remains relatively constant across the range of frequencies critical to the analysis. The second frequency should be the closest rational number that aligns with the relationship between the predominant seismic signal and the base frequency.

Figure 22 displays the alpha (α) and beta (β) damping parameters for a fundamental period of 2.00 seconds. Analysis of the Fourier spectrum of the three signals considered for dynamic analyses reveals that the Iwate signal has the highest frequency content closest to the fundamental frequencies of the Guavio dam, making it particularly relevant for these studies.

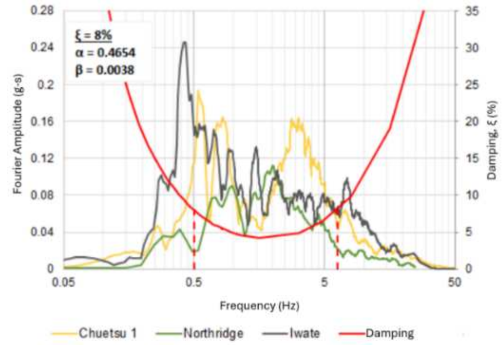

Figure 22. Rayleigh's damping parameters for a fundamental period of 2.00 seconds.

1.3. EARTHQUAKE-INDUCED DEFORMATION

The accelerations in the crest of the dam for the Iwate ground motion are presented in Figure 23, where it is estimated that the acceleration in the Strait varies between 4,05 m/s2 and 5,18 m/s2, these accelerating values correspond to amplification factors between 1,02 and 1,30, presenting the greatest amplification for the model with the longest fundamental period (T1 = 2,50 s) i.e. for the less rigid model. As with the previous results, the highest accelerations are presented for the model with a period close to the predominant signal period, in this case a period of 2.50 s.

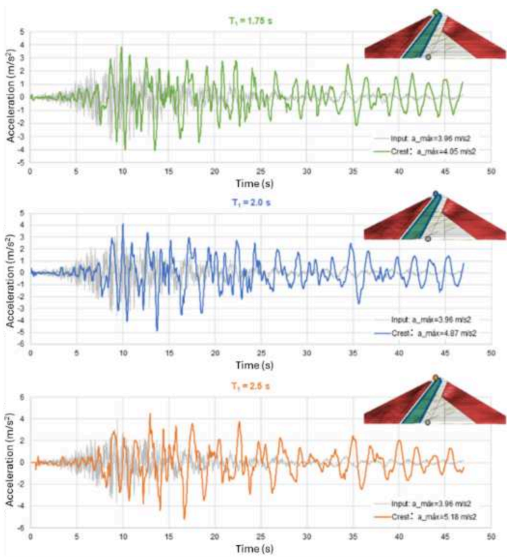

Figure 23. Horizontal acceleration at the model's crest and base - Iwate signal.

The displacements and settlements in the crest for the Iwate ground motion are presented in Figure 24, whereas the largest displacement and settlement is found in the model with a period of 1.75 seconds, for this case reaching settlement of up to 90 cm and total displacements of 1.0 m. Dynamic analysis with this ground motion produces displacements in a direction perpendicular to the axis of the dam (direction x in the numerical model) greater than 40 cm for the three periods considered in the analyses, which being greater to those estimated with the other input ground motions do not pose a problem for the stability and operation of the dam.

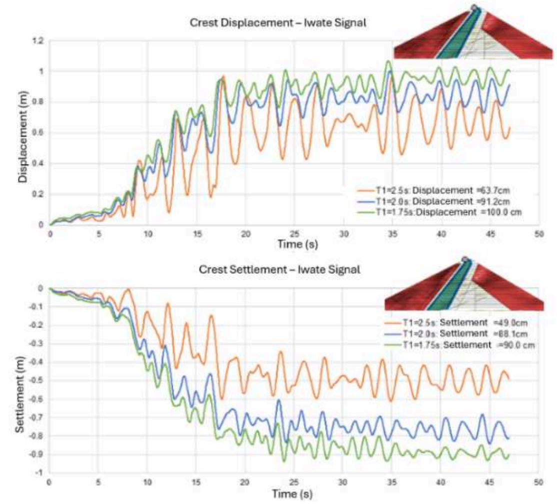

Figure 24. Displacement and settlement in the crest of Dam - Iwate Signal.

Figure 25 presents the estimated settlements with the numerical model for the three analytical signals and the three critical periods considered. It is estimated that the maximum settlements are presented for the most stiffness model (T1=1.75 s) and for the Iwate ground motion, which has the highest frequency content in the range of periods of the Guavio dam. The total settlements and displacements estimated with both the numerical model and the simplified methodology of Makdisi and Seed are in all cases values less than 120 cm, which meets the safety requirements (CDA, 2013) for the scenario associated with the SEE (Safety Evaluation Earthquake) verification scenario taking into account the 10 m free edge that the dam currently has for the condition of dam at the maximum normal level of operation (FSL) at the EL. 1630,00 masl.

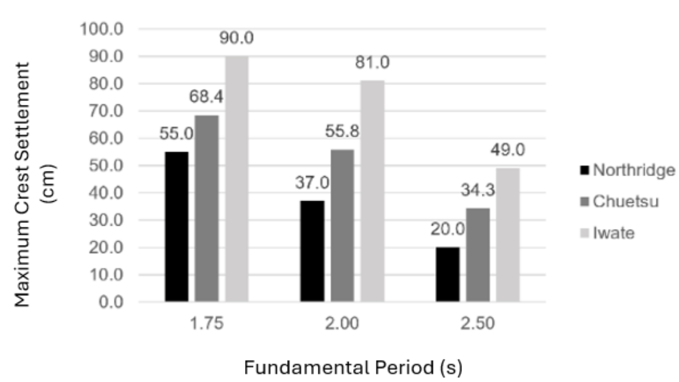

Figure 25. Seismically induced settlements on the dam crest.

2. DISCUSSION

The Guavio dam of the Guavio Hydroelectric Power Plant is a structure with 32 years of operation, with a good knowledge of its geometry and the geotechnical properties of the materials that make it (physical, cutting resistance, permeability and deformability) that are supported by the reports and tests carried out during its design and construction phase. This was supplemented by the MASW geophysical tests carried out at this stage of the study, which validated the dynamic properties of the core and rockfill shells. All the above information was the input for the numerical models of slope stability analysis with LEM and finite elements developed with which the dynamic response of the dam to the SEE (Safety Evaluation Earthquake) request was evaluated and are discussed below, with an analysis focused on concluding the level of vulnerability of the Guavio dam in the event of the verification earthquake.

The analyses developed in the present study can be grouped into three main categories:

- Simplified analysis or pseudo-static approximations.
- Simplified dynamic analysis such as the Makdisi and Seed method.
- Complex dynamic analysis, through numerical models of finite elements, considers the dam as a continuous and deformable medium, which responds to the characteristics of the seismic signal.

The pseudo-static Safety Factors (considering 50% of the verification earthquake PGA) obtained for both the upper and lower waters were higher than one (1,0) with values ranging between 1.38 and 1.40 for a total potential failure of the entire back and between 1.24 and 1.55 for an inter-ramp potential failures area.

The second type of analysis (simplified analysis implementing the Makdisi and Seed methodology) allowed to estimate maximum seismically-induced deformations of the order of 120 cm and 90 cm when using the median curve of deformation induced proposed by Makdisi and Seed. The greatest amplification effects are presented for the condition in which the high range of wave speeds for the dam body was analyzed, in which a greater coincidence is presented in the frequency content of the input signals and the estimated fundamental modes for the Guavio dam.

In the dynamic analyses implementing the methodology of finite elements, maximum seismic settlements of the order of 90 cm were estimated, which was estimated for the model with the highest rigidity analyzed which has an associated fundamental period of 1.75 seconds. In general terms, the results found expressed by the magnitude of the estimated maximum induced seismic settlements and the greater amplification for the lowest fundamental period state analyzed (1,75 seconds) is consistent with the results of the simplified analyses, with which it can be concluded that the expected seismic settlement for the Guavio dam would be less than 1.2 m.

3. CONCLUSSION

The Guavio dam of the Guavio Hydroelectric Power Plant meets the safety requirements (CDA, 2013) for the scenario associated with the SEE (Safety Evaluation Earthquake) earthquake, as the maximum expected settlement of the creek, which is of the order of 120 cm, is covered and can be safely absorbed by its current free edge of 10 m, which still remains the same as the design, since the 2 m camber that was left at the end of construction corresponds almost exactly to the settlements registered for the upstream above the crest. In fact, the central impermeable core also has a 2 m camber inside it, as the crest of it is located between EL. 1639 and 1640 masl, which is between 1 m and 2 m above the theoretical level of the EL.1638 masl. In this order of ideas, the lower sector of the dam core could be today between EL. 1637 and 1638 masl, which for the Full Supply Level (FSL) in the EL.1630 masl corresponds to a free edge of the waterproof zone of at least 7 m, with which the maximum settlement of 1.20 m expected in the event of an earthquake can be safely absorbed.

4. ACKNOWLEDGEMENTS

The authors express our gratefulness to ENEL owner of Guavio Hydro Power (Alberto Lleras Camargo Dam), for granting the permission to publish this article.

5. REFERENCES

Barton N. (2016). Non-linear shear strength for rock, rock joints, rockfill and interfaces. Innovative Infrastructure Solutions. Vol. 30, Issue 1.

Bozorgnia Y. and Campbell K.W. (2004). The vertical-to-horizontal response spectral ratio and tentative procedures for developing simplified v/h and vertical design spectra, Journal of Earthquake Engineering, 8:2, 175-207.

Canadian Dam Association -CDA-. (2013). Dam safety guidelines. 2013 Edition. ISBN 978.0.9936319.0.

Cheng Y., Yip C., (2007). Three‐dimensional asymmetrical slope stability analysis extension of Bishop's, Janbu's, and Morgenstern–Price's techniques. J. Geotech. Geoenviron. 133 (12), 1544–1555.

Huang, C.C., Tsai, C.C., Chen, Y.H., (2002). Generalized method for three‐dimensional slope stability analysis. J. Geotech. Geoenviron. 128 (10), 836–848.

Hungr O., (1994). "A general limit equilibrium model for three-dimensional slope stability analysis". Discussion of an article by L. Lam and D.G. Fredlund. Canadian Geotechnical Journal, 31: 793-795.

Hungr, O., (2001). "CLARA-W: Slope stability analysis in two or three dimensions for microcomputers". O. Hungr Geotechnical Research Inc., Vancouver, B. C. Canada.

INGETEC (2019). Estudio de amenaza sísmica central hidroeléctrica del Guavio. Bogotá D.C.

Makdisi F. and Seed H. (1979). Simplified procedure for estimating dam and embankment earthquake-induced deformations. Journal of Geotechnical Engineering 104(7): 849–867.

Marulanda, A., Marulanda, C.. and Hinks, J. 2023. Earthquake Engineering
for Dams and Reservoirs. *Chapter 7 - Seismic design of rockfill dams*. 65-103. Emerald Publishing Limited.

Montes N. and Sandoval A. (2001). Base de Datos de Fallas Activas de Colombia - Compilación Bibliográfica. INGEOMINAS. Bogotá. 331 pages.

Mucciarelli M. and Gallipoli M. (2004). The HVSR technique from microtremor to strong motion: empirical and statistical considerations. 13th World Conference on Earthquake Engineering Vancouver, B.C., Canada August 1-6, 2004 Paper No. 45.

Nakamura Y., (1989). A method for dynamic characteristics estimations of subsurface using microtremors on the ground surface, QR RTRI, 30, 25-33, 1989.

Silva C, Marsal R. (1970). Pruebas de compresión triaxial y unidimensional - Enrocamiento de la presa La Esmeralda Proyecto Chivor, Colombia.

Zangar C. N. (1952). Hydrodynamic pressures on dams due to horizontal earthquake effects (No. 11). Technical Information Office.